



HAL
open science

LETTER Conditional and residual trends of singular hot days in Europe

Aglaé Jézéquel, Emanuele Bevacqua, Fabio D'andrea, Soulivanh Thao, Robert Vautard, Mathieu Vrac, Pascal Yiou

► **To cite this version:**

Aglaé Jézéquel, Emanuele Bevacqua, Fabio D'andrea, Soulivanh Thao, Robert Vautard, et al.. LETTER Conditional and residual trends of singular hot days in Europe. Environmental Research Letters, 2020, 15 (6), pp.064018. 10.1088/1748-9326/ab76dd . hal-02877736

HAL Id: hal-02877736

<https://hal.sorbonne-universite.fr/hal-02877736>

Submitted on 22 Jun 2020

HAL is a multi-disciplinary open access archive for the deposit and dissemination of scientific research documents, whether they are published or not. The documents may come from teaching and research institutions in France or abroad, or from public or private research centers.

L'archive ouverte pluridisciplinaire **HAL**, est destinée au dépôt et à la diffusion de documents scientifiques de niveau recherche, publiés ou non, émanant des établissements d'enseignement et de recherche français ou étrangers, des laboratoires publics ou privés.

LETTER • OPEN ACCESS

Conditional and residual trends of singular hot days in Europe

To cite this article: Aglaé Jézéquel *et al* 2020 *Environ. Res. Lett.* **15** 064018

View the [article online](#) for updates and enhancements.



LETTER


Conditional and residual trends of singular hot days in Europe

OPEN ACCESS

RECEIVED
29 October 2019REVISED
12 February 2020ACCEPTED FOR PUBLICATION
17 February 2020PUBLISHED
27 May 2020

Original content from this work may be used under the terms of the [Creative Commons Attribution 4.0 licence](#).

Any further distribution of this work must maintain attribution to the author(s) and the title of the work, journal citation and DOI.

Aglaé Jézéquel^{1,2} , Emanuele Bevacqua³ , Fabio d'Andrea¹, Soulivanh Thao⁴ , Robert Vautard⁴ ,
Mathieu Vrac⁴ and Pascal Yiou⁴¹ LMD/IPSL, ENS, PSL Université, École Polytechnique, Institut Polytechnique de Paris, Sorbonne Université, CNRS, Paris, France² Ecole des Ponts, Marne-la-Vallée, France³ Department of Meteorology, University of Reading, Reading, United Kingdom⁴ Laboratoire des Sciences du Climat et de l'Environnement, UMR8212 CEA-CNRS-UVSQ, IPSL & U Paris-Saclay, 91191 Gif-sur-Yvette, FranceE-mail: aglae.jezequel@lmd.ens.fr**Keywords:** climate change, extreme events, thermodynamics, dynamics, attributionSupplementary material for this article is available [online](#)**Abstract**

The influence of anthropogenic climate change on both mean and extremely hot temperatures in Europe has been demonstrated in a number of studies. There is a growing consensus that high temperature extremes have increased more rapidly than the regional mean in central Europe, while the difference between extreme and mean trends is not significant in other European regions. However, it is less clear how to quantify the changes in different processes leading to heat extremes. Extremely hot temperatures are associated to a large extent with specific types of atmospheric circulation. Here we investigate how the temperature associated with atmospheric patterns leading to extremely hot days in the present could evolve in the future. We propose a methodology to calculate conditional trends tailored to the circulation patterns of specific days by computing the evolution of the temperature for days with a similar circulation to the day of interest. We also introduce the concept of residual trends, which compare the conditional trends to regional mean temperature trends. We compute these trends for two case studies of the hottest days recorded in two different European regions (corresponding to the heat-waves of summer 2003 and 2010). We use the NCEP reanalysis dataset, an ensemble of CMIP5 models, and a large ensemble of a single coupled model (CESM), in order to account for different sources of uncertainty. We also evaluate how bias correction of climate simulations influences the results.

1. Introduction

Anthropogenic climate change has a clear influence on European summer temperature (Bindoff *et al* 2013). A number of studies have shown an increase in both the observed and projected European temperature mean and extremes (Seneviratne *et al* 2012, Bindoff *et al* 2013, Seneviratne *et al* 2016). There is also a growing consensus that trends on extreme summer heat events are stronger than trends on seasonal averages of regional temperatures in Central Europe in both observations (Della-Marta *et al* 2007, Lorenz *et al* 2019) and climate model projections (Fischer *et al* 2012, Lustenberger *et al* 2014, Cattiaux *et al* 2015), with no significant difference in other European regions. Higher trends on extreme summer temperature than in the average regional summer temperatures have

been explained by changes in land-surface feedback (Seneviratne *et al* 2006, Douville *et al* 2016), thermal advection (Holmes *et al* 2016), and cloud cover (Tang *et al* 2012). Understanding the evolution of the processes leading to extreme temperatures is however partially hindered by the differences between available climate model simulations (Fischer and Schär 2008), which can be caused by both internal variability and different model parameterizations of physical processes. One way to move forward is to disentangle the dynamical and non-dynamical contributions to an extreme event, and to study the evolution of one or both of these contributions (Trenberth *et al* 2015, Shepherd 2016, Vautard *et al* 2016, Yiou *et al* 2017).

Indeed, a large part of the variability of the European climate is governed by atmospheric dynamics

conveyed in the atmospheric circulation fluctuations. For example, high temperatures are related to specific types of circulation, mostly long-lasting anticyclonic anomalies called blockings (e.g. Cassou *et al* 2005, Pfahl and Wernli 2012, Sousa *et al* 2018). Jézéquel *et al* (2018b) showed that the distribution of temperature for circulation patterns similar to those of observed heatwaves—also called analogs—is a subset of the higher temperature values of the total temperature distribution.

In the context of climate change, this leads to two questions. First, what is the influence of climate change on circulation types leading to extreme temperatures? The evolution of mid-latitude atmospheric circulation is uncertain (Shepherd 2014, Xie *et al* 2015, Yao *et al* 2017, Collins *et al* 2018, Luo *et al* 2018). In particular, evidences on the changes in the occurrence of summer blockings seem to diverge (Ruti *et al* 2014, Coumou *et al* 2015, Peings *et al* 2017). In Jézéquel *et al* (2018a), we introduced the concept of dynamical trends, to evaluate whether the frequency of these circulation patterns was affected by climate change and found contrasting results for two case studies. The present article will address the second question: how does climate change affect the temperature associated with a given circulation type that led to an extreme temperature in the current climate?

Because of the uncertainty on the atmospheric circulation response to climate change, it is easier to extract a signal in response to climate change while fixing the dynamical part of that signal. The signal over noise ratio generally increases after dynamical adjustment (Wallace *et al* 1995). Dynamical adjustment consists in extracting the non-circulation related signal from a time series. It can be achieved using a variety of techniques, for example analog-based techniques (e.g. Deser *et al* 2016, Lehner *et al* 2017, Merrifield *et al* 2017) or regression-based techniques (e.g. Smoliak *et al* 2015, Saffioti *et al* 2016). It has been used for several purposes, including explaining the warming hiatus (Smoliak *et al* 2015), or explaining the spread between different model projections (Saffioti *et al* 2017).

To our knowledge, there are no studies applying dynamical adjustment techniques to a specific circulation type. Our objective in this article is hence to propose a methodology to do that, by introducing *conditional trends* and *residual trends*. Given a circulation type leading to an extreme temperature in the current climate, conditional trends evaluate how the temperature associated with this circulation changes in response to changes in anthropogenic emissions. Residual trends assess how large this change is compared with the mean regional change of the overall temperature distribution. In section 2, we introduce the datasets and we define both types of trends. In section 3, we present the result of these methodologies applied to the same two case studies used by Jézéquel *et al* (2018a): 13th August 2003 in Western Europe

(hereafter referred to as 2003) and 7th August 2010 in Russia (hereafter referred to as 2010). We discuss the results in section 4.

2. Data and Methods

2.1. Datasets

In this study, we use daily surface temperature and, as a proxy for the mid-latitude atmospheric circulation, geopotential height at 500 hPa (Z500). As we focus on the summer season (June–July–August: JJA), Z500 presents the advantage over sea level pressure that it is not affected by heat lows, which blur the circulation patterns by superimposing low pressure systems on high pressure systems associated with the blockings that generally cause high temperatures in Europe (see more details on this in Jézéquel *et al* 2018b). As in Jézéquel *et al* (2018a), we use daily values of Z500 over two European subregions: [20W–20E; 40N–60N] and [10E–68E; 45N–70N], respectively called hereafter Western Europe (WE-Z500) and Russia (RU-Z500), as shown in figure 1. To avoid capturing the mean Z500 trend associated to the surface temperature trend, we remove a spatially uniform Z500 trend, calculated on the mean seasonal (JJA) spatial average on the region of interest. Since there is no reason for the trend to be linear, we use a cubic smoothing spline. We heuristically chose a high smoothing parameter ($spar = 0.9$ using the R function `smoothing.spline`) to limit the number of degrees of freedom, in order to preserve natural interannual variability (more details on the reasoning behind this detrending are provided in Jézéquel *et al* 2018a).

For temperature, we use daily spatial averages over smaller regions: [5W–20E; 36N–50N] (WE-T in figure 1) for 2003 (following Jézéquel *et al* 2018b) and [35E–55E; 50N–60N] (RU-T in figure 1) for 2010 (following Dole *et al* 2011). We remove the seasonal cycle from the temperature times series. The seasonal cycle was computed with a cubic smoothing spline calculated from the daily calendar day average for each dataset. We apply no tension to this spline (we set the smoothing spline parameter in R to $spar = 0$). Removing the seasonal cycle allows us to filter out the difference in temperature between analogs picked from days at the beginning, in the middle or at the end of the summer. By doing this, we possibly ignore any potential changes of seasonality in the occurrence of analogs, which could have an influence on conditional trends.

In order to assess whether trends are detectable in the observations, we use the National Centers for Environmental Prediction/National Center for Atmospheric Research, NCEP/NCAR, reanalysis I dataset (Kalnay *et al* 1996) between 1950 and 2016 for Z500. Its horizontal resolution is $2.5^\circ \times 2.5^\circ$. For temperature, we use the E-OBS dataset (Cornes *et al* 2018) for the Western Europe region. Its resolution is

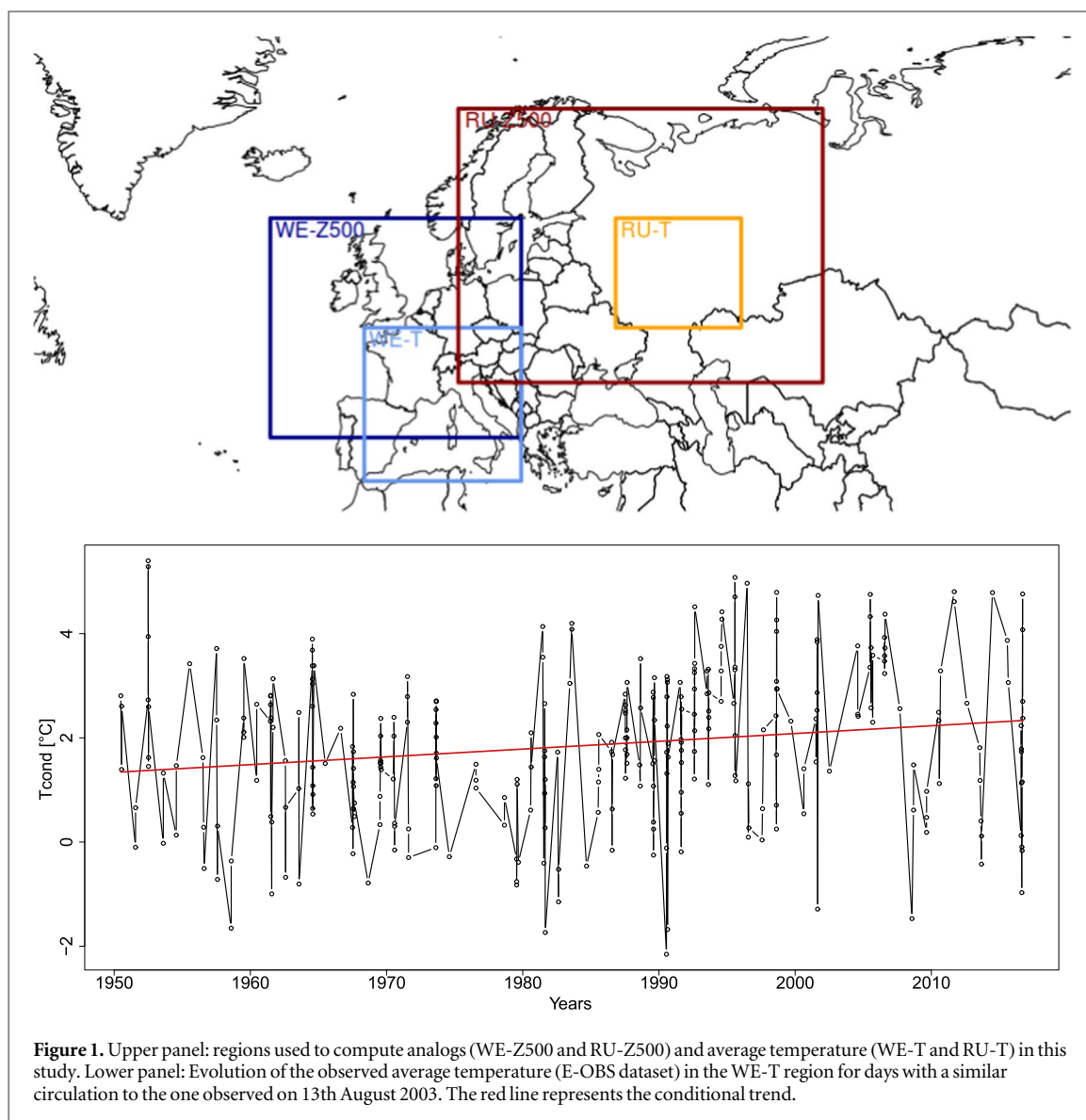


Figure 1. Upper panel: regions used to compute analogs (WE-Z500 and RU-Z500) and average temperature (WE-T and RU-T) in this study. Lower panel: Evolution of the observed average temperature (E-OBS dataset) in the WE-T region for days with a similar circulation to the one observed on 13th August 2003. The red line represents the conditional trend.

$0.25^\circ \times 0.25^\circ$. Since the Russian region we are interested in is not encompassed in the E-OBS region, we use the Berkeley Earth surface temperature (BEST) (Rohde *et al* 2013). Its resolution is $1^\circ \times 1^\circ$. The sensitivity to these choices is discussed later in the article.

To get a better idea of how conditional and residual trends could change in the future for different scenarios of greenhouse gases emissions, we rely on two ensembles of coupled climate models. The first ensemble consists of 16 models from the fifth Coupled Model Inter-comparison Project (CMIP5) (Taylor *et al* 2012, see model references and resolutions in the supplementary material of Jézéquel *et al* 2018a is available at stacks.iop.org/ERL/15/064018/mmedia). They cover the 1950–2100 period, with a historical simulation from 1950 to 2005 and RCP4.5 (Representative Concentration Pathway, van Vuuren *et al* 2011) and RCP8.5 scenarios from 2006 to 2100, respectively corresponding to medium and high emissions scenarios. The second ensemble consists of 30 runs of the Community Earth System Model large ensemble (CESM-LENS) (Kay *et al* 2015). The model horizontal resolution

is $1^\circ \times 1^\circ$. It covers the 1950–2100 period with a historical simulation for the 1950–2005 period and the RCP8.5 scenario from 2006 to 2100.

These two different ensembles allow us to evaluate the influence of both internal variability (through CESM) and uncertainty related to the choice of the model (through CMIP5) on the results. We concatenate historical runs over 1950–2005 with RCP8.5 runs over the 2006–2016 period. This allows the comparison with reanalysis data over the whole 1950–2016 period. Here, the choice of RCP8.5 is both coherent with observations and the only scenario available for CESM-LENS.

2.2. Conditional trends

We define *conditional trends* as trends of a variable of interest (here temperature) for a fixed circulation type. They are computed based on analogs of circulation of a single day of interest j . The first step is to select analog days in the same way as done for dynamical trends by Jézéquel *et al* (2018a). First, we define the analogs as

the subset of days S_j with a Euclidean distance to the circulation of the day of interest j below the 5th percentile of the distribution of summer days distances to the day of interest. This threshold is computed separately for each dataset, using the whole time series. We compute these distances between Z500 maps in the WE-Z500 and RU-Z500 regions defined above (more details on the methodology can be found in Jézéquel *et al* 2018a).

Second, we can deduce a series of temperature of these analogs from the temperature field T' , which has been previously deseasonalized on the entire annual temperature record. The conditional trends are defined as the regression coefficient a_{cond} , obtained when fitting a simple linear regression model, based on the least squares method, on the de-seasonalized daily temperatures time series $T'(t \in S_j)$:

$$T'(t \in S_j) = a_{cond} \cdot t + b_{cond} + \epsilon_{cond}(t), \quad (1)$$

where t is the time (in days), b_{cond} is the intercept term and $\epsilon_{cond}(t)$ is the error term. An example of the procedure applied to the E-OBS dataset for the 2003 case is shown in the lower panel of figure 1. We display a_{cond} in figure 2, with a 95% confidence interval computed for each dataset and each experiment (the formula to compute this confidence interval is given in section 8.3.7 of Von Storch and Zwiers 2001). We detect an increase (resp. decrease) of temperature for days with a similar circulation pattern when a_{cond} is significantly positive (resp. negative).

2.3. Residual trends

Conditional trends inform on the evolution of the temperature for a given circulation. However, conditional trends may differ from unconditional mean regional temperature trends. In order to assess potential differences between these unconditional and conditional trends, we define *residual trends*. To compute residual trends, we first calculate regional summer mean temperature trends over the two regions of interest, here WE-T and RU-T (see figure 1). They are computed using a cubic smoothing spline, in order to take into account the nonlinearity of the unconditional trend. Second, we subtract these unconditional trends $s(y)$, where y is the time (in years), from the daily analog temperature series, as:

$$T_{res}(t \in S_j) = T'(t \in S_j) - s(y). \quad (2)$$

Then we define residual trends, i.e. the linear trends of the detrended daily analog temperatures T_{res} as the linear regression coefficient a_{res} :

$$T_{res}(t \in S_j) = a_{res} \cdot t + b_{res} + \epsilon_{res}(t), \quad (3)$$

where the different terms and coefficient are defined as above.

Our calculation supposes that the analog days are spread out over the whole time period, which is verified on the data. They are however not uniformly distributed (since we found in Jézéquel *et al* 2018a some cases of significant changes in the frequency of

occurrence of the circulation of interest), which is reflected in the calculation of the confidence intervals. Besides, using linear trends has limitations, since there is no reason for the change to be linear. This means we will not capture all the characteristics of the trend. However, at this point we only want to test whether we detect significant trends, so the linear model should suffice for our purpose.

2.4. Bias correction

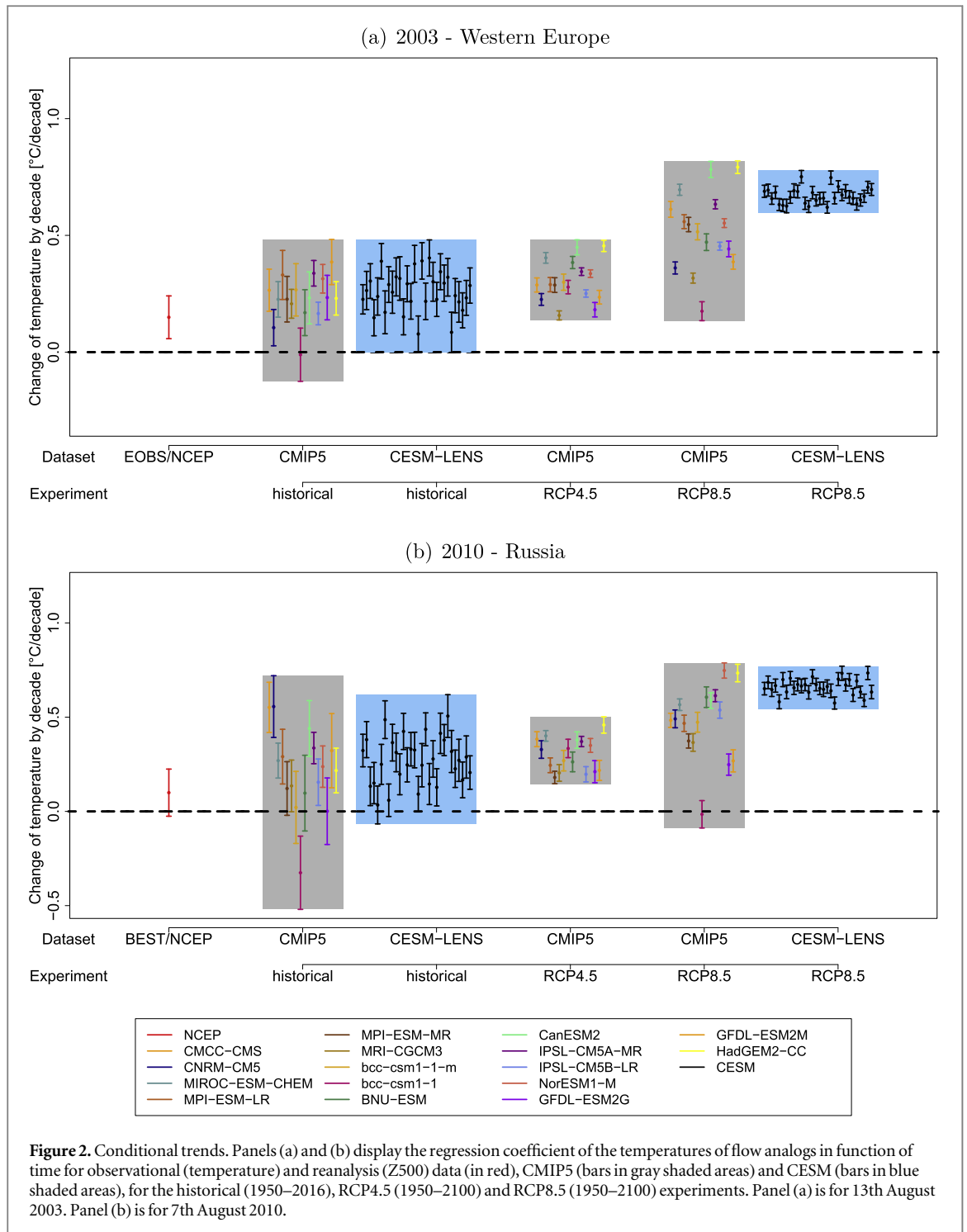
Models have biased representation of both temperature and Z500 (Dosio and Paruolo 2011, Cattiaux *et al* 2013, White and Toumi 2013). A few recent studies are advocating for the use of bias correction to account for models bias to study the influence of climate change on extreme weather events (e.g. Jeon *et al* 2016, Bellprat *et al* 2019). Here, we performed bias correction on both variables as a sensitivity test and checked whether and how it affects the results. For Z500, the detrending we systematically apply sets all the means to zero and hence results in a sort of bias correction of the average of the Z500 distribution. Similarly to what was done in Jézéquel *et al* (2018a), we compared the results between detrending, and three different types of normalization: a simple normalization (division by the standard deviation) gridpoint by gridpoint, another on the spatial mean of the Z500 field and a quantile-mapping (e.g. Panofsky and Brier 1958, Déqué 2007, Gudmundsson *et al* 2012). Since the normalization has a marginal influence on the results, we only present hereafter the results for detrended Z500.

For the temperature, we used the ‘cumulative distribution function-transform’ (CDF-t) method (Vrac *et al* 2012) applied to the deseasonalized summer daily temperature field, with 1950–2005 as the calibration period and 2006–2100 as the target period. The results obtained with and without bias correction are displayed and discussed in the following sections.

3. Results

3.1. Conditional trends without bias correction

Figure 2 displays the conditional trends associated to the 2003 and 2010 cases. For the historical period, most of the conditional trends are significantly positive (p -value < 0.05). For 2003, the observed conditional trend is significantly positive (p -value of 0.001). 15 out of 16 CMIP5 models and all the CESM runs reproduce this significant positive trend, although some trends are relatively large compared to the observed one. The trend computed for bcc-csm1-1 is not significant; this could be due to internal variability, since we only use one member by model. The NCEP conditional trend for 2010 is positive but not significant (p -value of 0.12). All models except bcc-csm1-1 detect positive trends, with differences between the models on the value and significance of these trends. The spread of



conditional trends for both the CMIP5 and the CESM ensemble is larger than for 2003, possibly pointing to a larger role of internal variability within the selected analogs in the RU region.

The width of the confidence intervals of each model and the internal variability between CESM runs drop for the 1950–2100 period. This shrinking does not stem from the increase in degrees of freedom related to the different lengths of the 1950–2016 and the 1950–2100 periods (obtained from a simple calculation based on the confidence interval formula from Von Storch and Zwiers 2001). It could be explained by

a larger role of internal variability in the historical period, while the climate change signal becomes clearer and more pronounced for a longer time period. The spread of the CMIP5 model ensemble (gray boxes) also decreases between the historical period and RCP4.5, but increases between RCP4.5 and RCP8.5. For 2003, the trends are all significantly positive (p -value < 0.5), approximately between 0.2 °C and 0.5 °C by decade for RCP4.5 and between 0.2 °C and 0.8 °C by decade for RCP8.5. All the trends increase between RCP4.5 and RCP8.5 except for *bcc-csm1-1*. For 2010, the trends are all significantly positive except

for bcc-csm1-1 for RCP8.5. They are approximately between $0.2\text{ }^{\circ}\text{C}$ and $0.5\text{ }^{\circ}\text{C}$ by decade for RCP4.5 and between $-0.1\text{ }^{\circ}\text{C}$ and $0.8\text{ }^{\circ}\text{C}$ by decade for RCP8.5.

The detection of significant positive trends both for the historical period and the projections is an expected result, since there is a clear trend on temperature extremes, which has been attributed to anthropogenic emissions (Bindoff *et al* 2013). The increase of these trends between the historical period and the projections, and between RCP4.5 and RCP8.5 is also characteristic of different potential levels of anthropogenic forcings. At least for 2003, the differences between models in the historical period is within the range of internal variability provided by the CESM ensemble. However, the inter-model spread for RCP8.5 cannot be explained only by internal variability. In the future climate under RCP8.5, model differences emerge clearly, which may be due to differences in climate sensitivity and/or to differences in the modeling of dynamics and of their link with temperature.

3.2. Residual trends without bias correction

Figure 3 displays the residual trends for the 2003 and 2010 cases. For 2003, the NCEP residual trend is significantly negative of approximately $-0.15\text{ }^{\circ}\text{C}$ by decade. For the historical period, most CMIP5 models (11 out of 16) detect negative residual trends, with differences in the significance and value of these trends. The models (from both the CMIP5 and CESM ensembles) generally underestimate this negative trend. For 2010, the NCEP residual trend is not significant and slightly negative (less than $-0.1\text{ }^{\circ}\text{C}$ by decade). The spread of residual trends for both the CMIP5 and the CESM ensemble is larger than for 2003.

The confidence intervals of each model, the internal variability between CESM runs, and the model spread all drop for the 1950–2100 period, which can be explained by the same reasoning as for the conditional trend case. For 2003, three (resp. eight) models detect a significant negative trend for RCP4.5 (resp. RCP8.5) and one (resp. two) model detects a significant positive trend with the rest being non-significant. For 2010, four (respectively five) models detect a significant negative trend for RCP4.5 (resp. RCP8.5) and three (resp. four) models detect a significant positive trend with the rest being non-significant. Different runs from the CESM ensemble detect significant trends from opposite signs, hinting at a large role of internal variability in residual trends, especially for the 2010 case.

Detecting negative residual trends and positive conditional trends, as is the case for the reanalysis dataset, implies that the regional trend is larger than the conditional trend. This means that for the type of circulation considered, temperature rises slower than the mean regional temperature. The inter-model spread of the residual trends of projections is about

half of the conditional trends spread, for 2003. This could imply that around half of the model uncertainties in the conditional trends comes from model uncertainties in the regional climate sensitivity. For 2010, this shrinking of the inter-model spread between conditional and residual trends is less pronounced, mainly because of outliers (BNU-ESM for RCP4.5 and bcc-csm1-1 for RCP8.5). It would be interesting to investigate how and why these two models differ from the others, but it is out of the scope of the present letter.

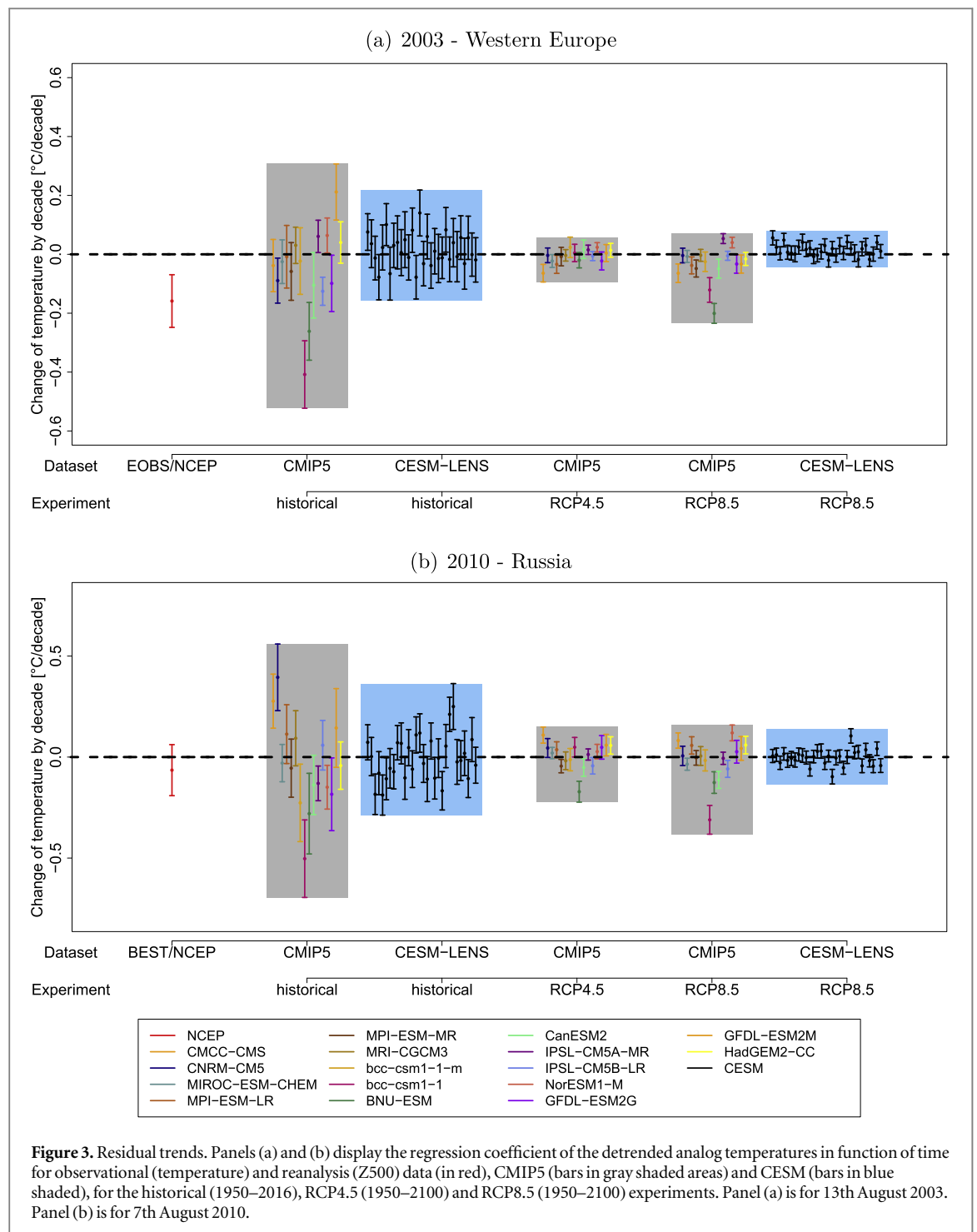
3.3. Quality of the datasets

3.3.1. Choice of reanalyses

Results can be sensitive to the choice of reanalyses (e.g. Alvarez-Castro *et al* 2018). For our study, we needed both temperature reanalysis and Z500 reanalysis datasets. The aim of our analysis required to use datasets spanning a relatively long time period in order to have enough data to calculate robust trends, and we wanted datasets that are regularly updated, so that this method could easily be applied to recent events. For Z500, only NCEP meets these criteria. However, it does not mean that NCEP is trustworthy. Figure 4 displays conditional and residual trends for 2003 and 2010 using different reanalysis datasets. We compared NCEP, and ERA20C for the 1950–2010 period, for both temperature and Z500. We found differences, a large part of which can be explained by the difference in Z500 fields. This result calls for caution in the interpretation of the results. We also found that analyzing data up to 2010 could have a large influence on results (e.g. for the conditional trend of the 2010 case study). For future studies, the ERA5 reanalysis (Copernicus Climate Change Service (C3S) 2017), which should cover the 1950–present period starting mid-2020, would be better suited. Since NCEP temperature is not very trustworthy (e.g. Sturaro 2003), we decided to use the NCEP Z500 field and to combine it with another temperature dataset. Figures S1 and S2 show the differences between conditional and residual trends computed using different temperature datasets: NCEP, BEST and E-OBS. The E-OBS and BEST datasets give qualitatively similar results for the WE-T region. The E-OBS dataset does not cover the RU-T region. The choice of the temperature dataset has more influence on conditional trends than on residual trends. This implies that it is more difficult to reproduce the observed unconditional trend on average temperature than the relative evolution of temperature for a fixed circulation type once the unconditional trend is removed, with the NCEP dataset.

3.3.2. Impact of bias correction

Figure S3 displays the difference between conditional trends calculated with temperature fields with and without bias correction using CDF-t for both 2003 and

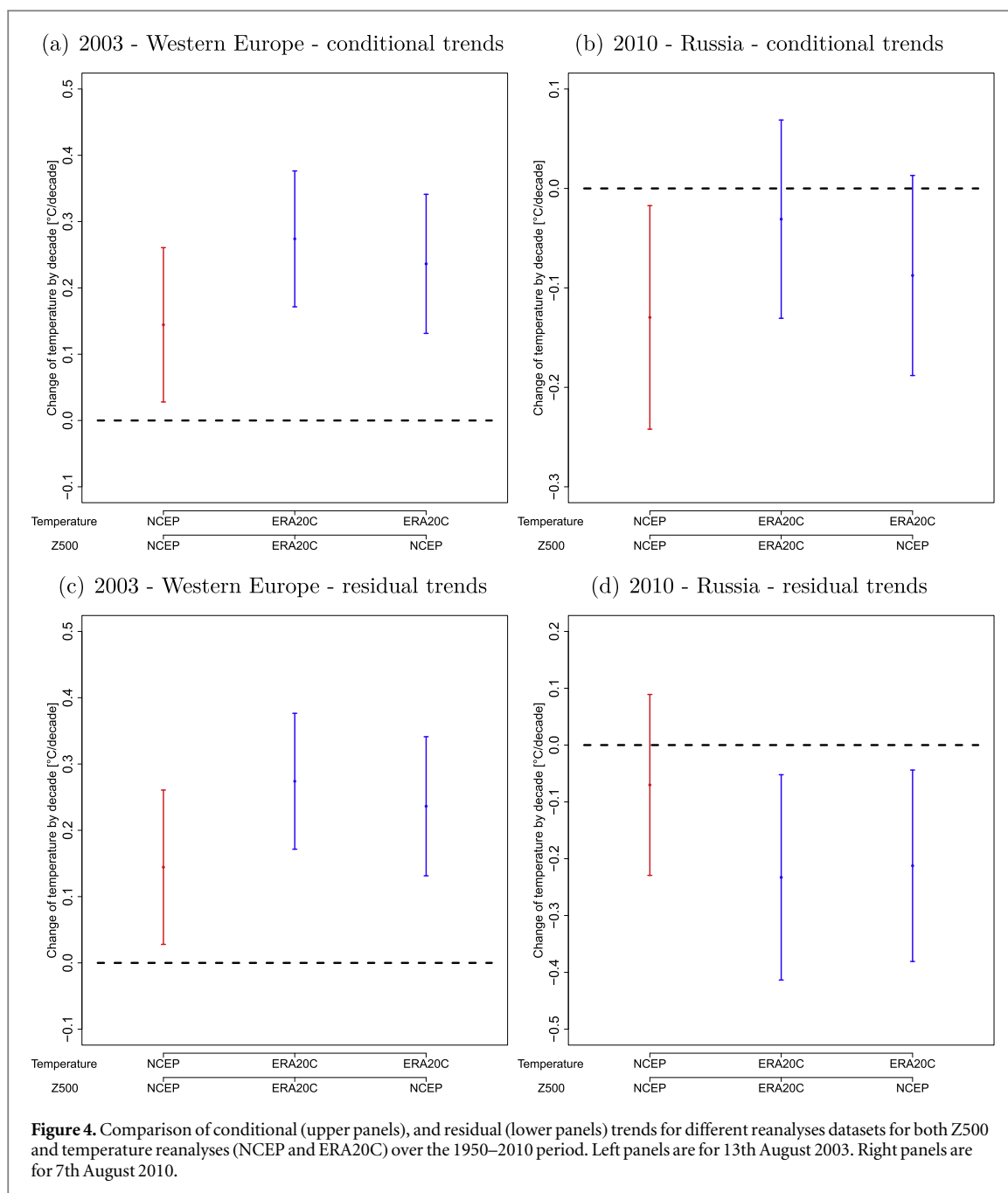


2010. Figure S4 displays the difference between residual trends calculated with temperature fields with and without bias correction using CDF-t for both 2003 and 2010. Bias correction has a bigger effect on projections than on the historical period. While some of the models are affected by the bias correction, with differences up to 0.3°C by decade, others are not. In some cases bias correction leads to an increase of conditional and residual trends, in others, it leads to a decrease. Bias correction generally leads to a wider multi-model range for both types of trends. The fact that bias correction has an influence on some of the results is a warning to take the results with caution. This calls for

further research to better understand which bias correction method is more adapted, as well as whether, how and why bias correction adds realism to the results. This research is out of the scope of this article.

4. Conclusions and discussion

In this paper, we introduce methodological tools to analyze how climate change affects the temperature associated with a given circulation type. We apply it to two case studies associated to two major heatwaves to demonstrate how the methodology works. One result



of our study is that conditional trends are significantly positive. This means that given the circulation pattern related to the 2003 and 2010 hottest days, there is a significant temperature increase both in the historical period and in the projections. Compared with the dynamical trends introduced in Jézéquel *et al* (2018a), the conditional trends calculated here contain a much stronger signal related to the increase of European summer temperatures associated with anthropogenic climate change. In particular, contrarily to dynamical trends, it is already possible to detect a significant trend over the historical period only.

The second part of our analysis shows that, over the historical period, for the 2003 (and to a lesser extent 2010) circulation pattern and associated temperature, almost half the models, and most importantly

the reanalyses detect a significantly negative residual trend. This implies that the rate of warming for the type of circulation related to the events analyzed here could be smaller than the mean regional rate of warming. A possible explanation would be a general decrease of the standard deviation of the unconditional temperature distribution. However, a number of studies have shown that the standard deviation of the temperature distribution in Central Europe actually increases (e.g. Vogel *et al* 2017, Wartenburger *et al* 2017, Lorenz *et al* 2019). The region we selected for 2003 is a part of Central Europe. We also did not find a significant decrease of unconditional variability in our datasets (not shown here). Therefore our results suggest that this change happens for the specific types of circulation we selected. Hot extremes in the future

could then be caused by different circulation patterns than the ones studied in this paper. A more complete study of residual trends applied to a large ensemble of circulation types (rather than just two specific circulation patterns) is needed to better understand how and why anthropogenic emissions may modify the link between circulation and temperature.

For the projections, the picture is more contrasted, as depending on the model and whether there is a bias correction or not, the residual trends can be significantly negative (down to approximately -0.5 °C by decade), not significant, or significantly positive (up to approximately $+0.4$ °C by decade). While residual trends should help to better understand whether circulation patterns leading to extreme heat in the historical period will also lead to extreme heat in the future, it is hard to conclude with the two examples we studied in the present article, since the models do not agree. The differences between models may for example arise from different representations of land-atmosphere feedbacks (e.g. representation of duration of anticyclonic blockings, of precipitation, or of vegetation). A better understanding of what differentiates these models would be necessary to analyze further the meaning of residual trends.

Another important feature of extreme heat is the duration of heat events and the stability of the atmospheric patterns leading to these events. The residual trends presented here only apply to daily circulation, which may be a limit in the case of extreme heat. It could however also be applied to shorter events, for example on different types of daily events strongly dependent on circulation patterns like precipitation extremes or storms Combined with the dynamical trends introduced in Jézéquel *et al* (2018a), conditional and residual trends provide tools to understand how an observed event is and will be affected by climate change. These trends, tailored to a specific event, could be used for extreme event attribution. One of the main advantages in obtaining these trends is that they are both easy to implement and cheap in computation time. They provide insight on the dynamical and thermodynamical contributions to extreme events, based on existing ensembles of simulations and complement the analyses of Vautard *et al* (2016).

Acknowledgments

We thank J Cattiaux for enlightening discussions. The two anonymous reviewers and the editor greatly helped improving the manuscript.

Data availability statement

No new data were created or analysed in this study.

ORCID iDs

Aglaé Jézéquel  <https://orcid.org/0000-0002-0957-3126>

Emanuele Bevacqua  <https://orcid.org/0000-0003-0472-5183>

Soulivanh Thao  <https://orcid.org/0000-0003-3461-8522>

Robert Vautard  <https://orcid.org/0000-0001-5544-9903>

References

- Alvarez-Castro M C, Faranda D and Yiou P 2018 Atmospheric dynamics leading to West European summer hot temperatures since 1851 *Complexity* **2018** 2494509
- Bellprat O, Guemas V, Doblas-Reyes F and Donat M G 2019 Towards reliable extreme weather and climate event attribution *Nat. Commun.* **10** 1732
- Bindoff N L *et al* 2013 *Detection and Attribution of Climate Change: From Global to Regional* (Cambridge: Cambridge University Press) ch 10
- Cassou C, Terray L and Phillips A S 2005 Tropical atlantic influence on European heat waves *J. Clim.* **18** 2805–11
- Cattiaux J, Douville H and Peings Y 2013 European temperatures in cmip5: origins of present-day biases and future uncertainties *Clim. Dyn.* **41** 2889–907
- Cattiaux J, Douville H, Schoetter R, Parey S and Yiou P 2015 Projected increase in diurnal and interdiurnal variations of European summer temperatures *Geophys. Res. Lett.* **42** 899–907
- Collins M *et al* 2018 Challenges and opportunities for improved understanding of regional climate dynamics *Nat. Clim. Change* **8** 101
- Copernicus Climate Change Service (C3S) 2017 ERA5: Fifth generation of ECMWF atmospheric reanalyses of the global climate *Copernicus Climate Change Service Climate Data Store (CDS)* Accessed: Jan 2020 (<https://cds.climate.copernicus.eu/cdsapp#!/home>)
- Cornes R C, van der Schrier G, van den Besselaar E J M and Jones P D 2018 An ensemble version of the e-obs temperature and precipitation data sets *J. Geophys. Res.: Atmos.* **123** 9391–409
- Coumou D, Lehmann J and Beckmann J 2015 The weakening summer circulation in the northern hemisphere mid-latitudes *Science* **348** 324–7
- Della-Marta P M, Luterbacher J, von Weissenfluh H, Xoplaki E, Brunet M and Wanner H 2007 Summer heat waves over western Europe 1880–2003, their relationship to large-scale forcings and predictability *Clim. Dyn.* **29** 251–75
- Déqué M 2007 Frequency of precipitation and temperature extremes over France in an anthropogenic scenario: model results and statistical correction according to observed values *Glob. Planet. Change* **57** 16–26
- Deser C, Terray L and Phillips A S 2016 Forced and internal components of winter air temperature trends over north america during the past 50 years: mechanisms and implications *J. Clim.* **29** 2237–58
- Dole R, Hoerling M, Perlwitz J, Eischeid J, Pegion P, Zhang T, Quan X W, Xu T and Murray D 2011 Was there a basis for anticipating the 2010 Russian heat wave? *Geophys. Res. Lett.* **38** 1–5
- Dosio A and Paruolo P 2011 Bias correction of the ENSEMBLES high-resolution climate change projections for use by impact models: evaluation on the present climate *J. Geophys. Res.* **116** D16106
- Douville H, Colin J, Krug E, Cattiaux J and Thao S 2016 Midlatitude daily summer temperatures reshaped by soil moisture under climate change *Geophys. Res. Lett.* **43** 812–8

- Fischer E M, Rajczak J and Schär C 2012 Changes in European summer temperature variability revisited *Geophys. Res. Lett.* **39** L19702
- Fischer E M and Schär C 2008 Future changes in daily summer temperature variability: driving processes and role for temperature extremes *Clim. Dyn.* **33** 917
- Gudmundsson L, Bremnes J B, Haugen J E and Engen-Skaugen T 2012 Downscaling RCM precipitation to the station scale using statistical transformations—a comparison of methods *Hydrol. Earth Syst. Sci.* **16** 3383–90
- Holmes C R, Woollings T, Hawkins E and de Vries H 2016 Robust future changes in temperature variability under greenhouse gas forcing and the relationship with thermal advection *J. Clim.* **29** 2221–36
- Jeon S, Paciorek C J and Wehner M F 2016 Quantile-based bias correction and uncertainty quantification of extreme event attribution statements *Weather Clim. Extremes* **12** 24–32
- Jézéquel A, Cattiaux J, Naveau P, Radanovics S, Ribes A, Vautard R, Vrac M and Yiou P 2018a Trends of atmospheric circulation during singular hot days in Europe *Environ. Res. Lett.* **13** 054007
- Jézéquel A, Yiou P and Radanovics S 2018b Role of circulation in European heatwaves using flow analogues *Clim. Dyn.* **50** 1145–59
- Kalnay E *et al* 1996 The NCEP/NCAR 40-year reanalysis project *Bull. Am. Meteorol. Soc.* **77** 437–71
- Kay J E *et al* 2015 The community earth system model (CESM) large ensemble project: a community resource for studying climate change in the presence of internal climate variability *Bull. Am. Meteorol. Soc.* **96** 1333–49
- Lehner F, Deser C and Terray L 2017 Toward a new estimate of time of emergence of anthropogenic warming: Insights from dynamical adjustment and a large initial-condition model ensemble *J. Clim.* **30** 7739–56
- Lorenz R, Stalhandske Z and Fischer E M 2019 Detection of a climate change signal in extreme heat, heat stress, and cold in Europe from observations *Geophys. Res. Lett.* **46** 8363–74
- Luo D, Chen X, Dai A and Simmonds I 2018 Changes in atmospheric blocking circulations linked with winter arctic warming: a new perspective *J. Clim.* **31** 7661–78
- Lustenberger A, Knutti R and Fischer E M 2014 Sensitivity of European extreme daily temperature return levels to projected changes in mean and variance *J. Geophys. Res.: Atmos.* **119** 3032–44
- Merrifield A, Lehner F, Xie S-P and Deser C 2017 Removing circulation effects to assess central US land-atmosphere interactions in the CESM large ensemble *Geophys. Res. Lett.* **44** 9938–46
- Panofsky H A and Brier G W 1958 *Some Applications of Statistics to Meteorology* (University Park, PA: College of Mineral Industries)
- Peings Y, Cattiaux J, Vavrus S and Magnusdottir G 2017 Late twenty-first-century changes in the midlatitude atmospheric circulation in the CESM large ensemble *J. Clim.* **30** 5943–60
- Pfahl S and Wernli H 2012 Quantifying the relevance of atmospheric blocking for co-located temperature extremes in the Northern Hemisphere on (sub-)daily time scales *Geophys. Res. Lett.* **39** L12807
- Rohde R, Muller R, Jacobsen R, Muller E, Perlmutter S, Rosenfeld A, Wurtele J, Groom D and Wickham C 2013 A new estimate of the average earth surface land temperature spanning 1753 to 2011 *Geoinfor. Geostat.: Overview* **7** 2
- Ruti P M, Dell'Aquila A and Giorgi F 2014 Understanding and attributing the Euro-Russian summer blocking signatures *Atmos. Sci. Lett.* **15** 204–10
- Saffioti C, Fischer E M, Scherrer S C and Knutti R 2016 Reconciling observed and modeled temperature and precipitation trends over Europe by adjusting for circulation variability *Geophys. Res. Lett.* **43** 8189–98
- Saffioti C, Fischer E M and Knutti R 2017 Improved consistency of climate projections over Europe after accounting for atmospheric circulation variability *J. Clim.* **30** 7271–91
- Seneviratne S I, Lüthi D, Litschi M and Schär C 2006 Land-atmosphere coupling and climate change in Europe *Nature* **443** 205–9
- Seneviratne S I *et al* (ed) 2012 *A Special Report of Working Groups I and II of the Intergovernmental Panel on Climate Change (IPCC)* (Cambridge: Cambridge University Press) pp 109–230
- Seneviratne S I, Donat M G, Pitman A J, Knutti R and Wilby R L 2016 Allowable CO₂ emissions based on regional and impact-related climate targets *Nature* **529** 477–83
- Shepherd T G 2014 Atmospheric circulation as a source of uncertainty in climate change projections *Nat. Geosci.* **7** 703–8
- Shepherd T G 2016 A common framework for approaches to extreme event attribution *Curr. Clim. Change Rep.* **2** 28–38
- Smoliak B V, Wallace J M, Lin P and Fu Q 2015 Dynamical adjustment of the northern hemisphere surface air temperature field: methodology and application to observations *J. Clim.* **28** 1613–29
- Sousa P M, Trigo R M, Barriopedro D, Soares P M M and Santos J A 2018 European temperature responses to blocking and ridge regional patterns *Clim. Dyn.* **50** 457–77
- Sturaro G 2003 A closer look at the climatological discontinuities present in the ncep/ncar reanalysis temperature due to the introduction of satellite data *Clim. Dyn.* **21** 309–16
- Tang Q, Leng G and Groisman P Y 2012 European hot summers associated with a reduction of cloudiness *J. Clim.* **25** 3637–44
- Taylor K E, Stouffer R J and Meehl G A 2012 An overview of CMIP5 and the experiment design *Bull. Am. Meteorol. Soc.* **93** 485–98
- Trenberth K E, Fasullo J T and Shepherd T G 2015 Attribution of climate extreme events *Nature Clim. Change* **5** 725–30
- van Vuuren D P *et al* 2011 The representative concentration pathways: an overview *Clim. Change* **109** 5
- Vautard R, Yiou P, Otto F E L, Stott P, Christidis N, van Oldenborgh G J and Schaller N 2016 Attribution of human-induced dynamical and thermodynamical contributions in extreme weather events *Environ. Res. Lett.* **11** 114009
- Vogel M M, Orth R, Cheruy F, Hagemann S, Lorenz R, Hurk B and Seneviratne S I 2017 Regional amplification of projected changes in extreme temperatures strongly controlled by soil moisture-temperature feedbacks *Geophys. Res. Lett.* **44** 1511–9
- Von Storch H and Zwiers F W 2001 *Statistical Analysis in Climate Research* (Cambridge: Cambridge University Press)
- Vrac M, Drobinski P, Merlo A, Herrmann M, Lavaysse C, Li L and Somot S 2012 Dynamical and statistical downscaling of the french mediterranean climate: uncertainty assessment *Nat. Hazards Earth Syst. Sci.* **12** 2769–84
- Wallace J M, Zhang Y and Renwick J A 1995 Dynamic contribution to hemispheric mean temperature trends *Science* **270** 780–3
- Wartenburger R, Hirschi M, Donat M G, Greve P, Pitman A J and Seneviratne S I 2017 Changes in regional climate extremes as a function of global mean temperature: an interactive plotting framework *Geosci. Model Dev.* **10** 3609–34
- White R H and Toumi R 2013 The limitations of bias correcting regional climate model inputs *Geophys. Res. Lett.* **40** 2907–12
- Xie S-P *et al* 2015 Towards predictive understanding of regional climate change *Nat. Clim. Change* **5** 921
- Yao Y, Luo D, Dai A and Simmonds I 2017 Increased quasi stationarity and persistence of winter ural blocking and eurasian extreme cold events in response to arctic warming: I. Insights from observational analyses *J. Clim.* **30** 3549–68
- Yiou P, Jézéquel A, Naveau P, Otto F E L, Vautard R and Vrac M 2017 A statistical framework for conditional extreme event attribution *Adv. Stat. Climatol., Meteorol. Oceanogr.* **3** 17–31